Chapter Number

Optimal Control of Transmission Power Management in Wireless Backbone Mesh Networks

Thomas Otieno Olwal[1,2,3], Karim Djouani[1,2], Barend Jacobus Van Wyk[1], Yskandar Hamam[1] and Patrick Siarry[2]
[1]*Tshwane University of Technology,*
[2]*University of Paris-Est,*
[3]*Meraka Institute, CSIR,*
[1,3]*South Africa*
[2]*France*

1. Introduction

The remarkable evolution of wireless networks into the next generation to provide ubiquitous and seamless broadband applications has recently triggered the emergence of Wireless Mesh Networks (WMNs). The WMNs comprise stationary Wireless Mesh Routers (WMRs) forming Wireless Backbone Mesh Networks (WBMNs) and mobile Wireless Mesh Clients (WMCs) forming the WMN access. While WMCs are limited in function and radio resources, the WMRs are expected to support heavy duty applications, that is, WMRs have gateway and bridge functions to integrate WMNs with other networks such as the Internet, cellular, IEEE 802.11, IEEE 802.15, IEEE 802.16, sensor networks, et cetera (Akyildiz & Wang, 2009). Consequently, WMRs are constructed from fast switching radios or multiple radio devices operating on multiple frequency channels. WMRs are expected to be self-organized, self-configured and constitute a reliable and robust WBMN which needs to sustain high traffic volumes and long online time. Such complex functional and structural aspects of the WBMNs yield additional challenges in terms of providing quality of services (QoS)(Li et al., 2009). Therefore, *the main objective of this investigation is to develop a decentralized transmission power management (TPM) solution maintained at the Link-Layer (LL) of the protocol stack for the purpose of maximizing the network capacity of WBMNs while minimizing energy consumption and maintaining fault-tolerant network connectivity*.

In order to maximize network capacity, this chapter proposes a scalable singularly-perturbed weakly-coupled TPM which is supported at the LL of the network protocol stack. Firstly, the WMN is divided into sets of unified channel graphs (UCGs). A UCG consists of multiple radios, interconnected to each other via a common wireless medium. A unique frequency channel is then assigned to each UCG. A multi-radio multi-channel (MRMC) node possesses network interface cards (NICs), each tuned to a single UCG during the network operation. Secondly, the TPM problems are modelled as a singular-perturbation of both energy and packet evolutions at the queue system as well as a weak-coupling problem, owing to the interference across adjacent multiple channels. Based on these models, an

optimal control problem is formulated for each wireless connection. Thirdly, differential Nash strategies are invoked to solve such a formulation. The optimization operation is implemented by means of an energy-efficient power selection MRMC unification protocol (PMMUP) maintained at the LL. The LL handles packet synchronization, flow control and adaptive channel coding (Iqbal & Khayam, 2009). In addition to these roles, the LL protocol effectively preserves the modularity of cross-layers and provides desirable WMN scalability (Iqbal & Khayam, 2009). Scalable solutions managed by the LL ensure that the network capacity does not degrade with an increase in the number of hops or nodes between the traffic source and destination. This is because the LL is strategically located just right on top of the medium access control (MAC) and just below the network layer. Message interactions across layers do not incur excessive overheads. As a result, dynamic transmission power executions per packet basis are expected to yield optimal power signals. Furthermore, if each node is configured with multiple MACs and radios, then the LL may function as a *virtual* MAC that hides the complexity of multiple lower layers from unified upper layers (Adya et al., 2004).

Finally, analytical results indicate that the optimal TPM resolves WMN capacity problems. Several simulation results demonstrate the efficacy of the proposed solution compared to those of recently studied techniques (Olwal et al., 2010**b**). The work in (Olwal et al., 2010**b**), furnishes an extensive review of the TPM schemes. In this chapter, however, only key contributions related to the MRMC LL schemes are outlined.

2. Related work

In order to make such MRMC configurations work as a single wireless router, a *virtual* medium access control (MAC) protocol is needed on top of the legacy MAC (Akyildiz & Wang, 2009). The virtual MAC should coordinate (unify) the communication in all the radios over multiple non-overlapping channels (Maheshwari et al., 2006). The first Multi-radio unification protocol (MUP) was reported in (Adya et al., 2004). MUP discovers neighbours, selects the network interface card (NIC) with the best channel quality based on the round trip time (RTT) and sends data on a pre-assigned channel. MUP then switches channels after sending the data. However, MUP assumes power unconstrained mesh network scenarios (Li et al., 2009). That is, mesh nodes are plugged into an electric outlet. MUP utilizes only a single selected channel for data transmission and multiple channels for exchanging control packets at high power.

Instead of MUP, this chapter considers an energy-efficient power selection multi-radio multi-channel unification protocol (PMMUP) (Olwal et al., 2009**a**). PMMUP enhances the functionalities of the original MUP. Such enhancements include: an energy-aware efficient power selection capability and the utilization of parallel radios over power controlled non overlapping channels to send data traffic simultaneously. That is, PMMUP resolves the need for a single mesh point (MP) node or wireless mesh router (WMR) to access mesh client network and route the backbone traffic at the same time (Akyildiz & Wang, 2009). Like MUP, the PMMUP requires no additional hardware modification. Thus, the PMMUP complexity is comparable to that of the MUP. PMMUP mainly coordinates local power optimizations at the NICs, while NICs measure local channel conditions (Olwal et al., 2009**b**). Several research papers have demonstrated the significance of the multiple frequency channels in capacity enhancement of wireless networks (Maheshwari et al., 2006; Thomas et al., 2007; Wang et al., 2006; Olwal et al., 2010**b**). While introducing the TPM

design in such networks, some solutions have guaranteed spectrum efficiency against multiple interference sources (Thomas et al., 2007; Wang et al., 2006; Muqattash & Krunz, 2005), while some offer topology control mechanisms (Zhu et al., 2008; Li et al., 2008). Indeed, still other solutions have tackled cross-layer resource allocation problems (Merlin et al., 2007; Olwal et al., 2009**a**; 2009**b**).

In the context of interference mitigation, Maheshwari et al. (2006) proposed the use of multiple frequency channels to ensure conflict-free transmissions in a physical neighbourhood so long as pairs of transmitters and receivers can tune to different non-conflicting channels. As a result, two protocols have been developed. The first is called extended receiver directed transmission (xRDT) while the second is termed the local coordination-based multi-channel (LCM) MAC protocol. While the xRDT uses one packet interface and one busy tone interface, the LCM MAC uses a single packet interface only. Through extensive simulations, these protocols yield superior performance relative to the control channel based protocols (Olwal et al., 2010**b**). However, issues of optimal TPM for packet and busy tone exchanges remained untackled. Thomas et al. (2007) have presented a cognitive network approach to achieve the objectives of power and spectrum management. These researchers classified the problem as a two phased non-cooperative game and made use of the properties of potential game theory to ensure the existence of, and convergence to, a desirable Nash Equilibrium. Although this is a multi-objective optimization and the spectrum problem is NP-hard, this selfish cognitive network constructs a topology that minimizes the maximum transmission power while simultaneously using, on average, less than 12% extra spectrum, as compared to the ideal solution.

In order to achieve a desirable capacity and energy-efficiency balance, Wang et al. (2006) considered the joint design of opportunistic spectrum access (i.e., channel assignment) and adaptive power management for MRMC wireless local area networks (WLANs). Their motivation has been the need to improve throughput, delay performance and energy efficiency (Park et al., 2009; Li et al., 2009). In order to meet their objective, Wang et al. (2006) have suggested a power-saving multi-channel MAC (PSM-MMAC) protocol which is capable of reducing the collision probability and the wake state of a node. The design of the PSM-MMAC relied on the estimation of the number of active links, queue lengths and channel conditions during the ad hoc traffic indication message (ATIM) window. In terms of a similar perspective, Muqattash and Krunz (2005) have proposed POWMAC: a single-channel power-control protocol for throughput enhancement. Instead of alternating between the transmission of control (i.e., RTS-CTS) and data packets, as done in the 802.11 scheme (Adya et al., 2004), POWMAC uses an access window (AW) to allow for a series of RTS-CTS exchanges to take place before several concurrent data packet transmissions can commence. The length of the AW is dynamically adjusted, based on localized information, to allow for multiple interference-limited concurrent transmissions to take place in the same vicinity of a receiving terminal. However, it is difficult to implement synchronization between nodes during the access window (AW). POWMAC does not solve the interference problem resulting from a series of RTS-CTS exchanges.

In order to address MRMC topology control issues, Zhu et al. (2008) proposed a distributed topology control (DTC) and the associated inter-layer interfacing architecture for efficient channel-interface resource allocation in the MRMC mesh networks. In DTC, channel and interfaces are allocated dynamically as opposed to the conventional TPMs (Olwal et al., 2010**b**). By dynamically assigning channels to the MRMC radios, the link connectivity, topology, and capacity are changed. The key attributes of the DTC include routing which is agnostic but

traffic adaptive, an ability to multiplex channel over multiple interfaces and the fact that it is fairly PHY/MAC layer agnostic. Consequently, the DTC can be integrated with various mesh technologies in order to improve capacity and delay performance over that of single-radio and/or single-channel networks (Olwal et al., 2010**b**). A similar TPM mechanism that solves the strong minimum power topology control problem has been suggested by Li et al. (2008). This scheme adjusts the limited transmission power for each wireless node and finds a power assignment that reserves the strong connectivity and achieves minimum energy costs. In order to solve problems of congestion control, channel allocation and scheduling algorithm for MRMC multi-hop wireless networks, Merlin et al. (2007) formulated the joint problem as a maximization of a utility function of the injected traffic, while guaranteeing stability of queues. However, due to the inherent NP-hardness of the scheduling problem, a centralized heuristic was used to define a lower bound for the performance of the whole optimization algorithm. The drawback is, however, that there are overheads associated with centralized techniques unless a proper TPM scheme is put in place (Akyildiz & Wang, 2009).
In Olwal et al. (2009**a**), an autonomous adaptation of the transmission power for MRMC WMNs was proposed. In order to achieve this goal, a power selection MRMC unification protocol (PMMUP) that coordinates Interaction variables (IV) from different UCGs and Unification variables (UV) from higher layers was then proposed. The PMMUP coordinates autonomous power optimization by the NICs of a MRMC node. This coordination exploits the notion that the transmission power determines the quality of the received signal expressed in terms of signal-to-interference plus ratio (SINR) and the range of a transmission. The said range determines the amount of interference a user creates for others; hence the level of medium access contention. Interference both within a channel or between adjacent channels impacts on the link achievable bandwidth (Olwal et al., 2009**b**).
In conclusion, the TPM, by alternating the dormant state and transmission state of a transceiver, is an effective means to reduce the power consumption significantly. However, most previous studies have emphasized that wake-up and sleep schedule information are distributed across the network. The overhead costs associated with this have not yet been thoroughly investigated. Furthermore, transmission powers for active connections have not been optimally guaranteed. This chapter will consequently investigate the problem of energy-inefficient TPM whereby nodes whose queue loads and battery power levels are below predefined thresholds are allowed to doze or otherwise participate voluntarily in the network. In particular, a TPM scheme based on singular perturbation in which queues on different or same channels evolve at different time-scales compared to the speed of transmission energy depletions at the multiple radios, is proposed (Olwal et al., 2010**a**). The new TPM scheme is also adaptive to the non orthogonal multi-channel problems caused by the diverse wireless channel fading. As a result, this paper provides an optimal control to the TPM problems in backbone MRMC wireless mesh networks (WMNs).
The rest of this chapter is organised as follows: The system model is presented in section 3. Section 4 describes the TPM scheme. In section 5, simulation tests and results are discussed. Section 6 concludes the chapter and furnishes the perspectives of this research.

3. System model

3.1 Unified channel graph model

Consider a wireless MRMC multi-hop WBMN assumed operating under dynamic channel conditions (El-Azouzi & Altman, 2003). Let us assume that the entire WBMN is virtually

divided into $\|L\|$ UCGs, each with a unique non-overlapping frequency channel as depicted in Fig. 1. Further, let each UCG comprise $\|V\|=N_V$, NICs or radio devices that connect to each other, possibly via multiple hops (Olwal et al., 2009**a**). These transmit and receive NIC pairs are termed as network users within a UCG. It should further be noted that successful communication is only possible within a common UCG; otherwise inter-channel communication is not feasible. Thus, each multi-radio MP node or WMR is a member of at least one UCG. In practice, the number of NICs at any node, say node A denoted as $\|T_A\|$, is less than the number of UCGs denoted as $\|L_A\|$, associated with that node, i.e., $\|T_A\| < \|L_A\|$. If each UCG set is represented as $l \ \forall l \in L$, then the entire WBMN is viewed by the higher layers of the protocol stack as unions of all UCG sets, that is, $l_1 \cup l_2 \cup l_3 \cup \ldots \cup l_{\|L\|}$. Utilizing the UCG model, transmission power optimization can then be locally performed within each UCG while managed by the Link-Layer (LL). The multi-channel Link state information (LSI) estimates that define the TPM problem are coordinated by the LL (Olwal et al., 2009**b**). Through higher level coordination, independent users are fairly allocated shared memory, central processor and energy resources (Adya et al., 2004).

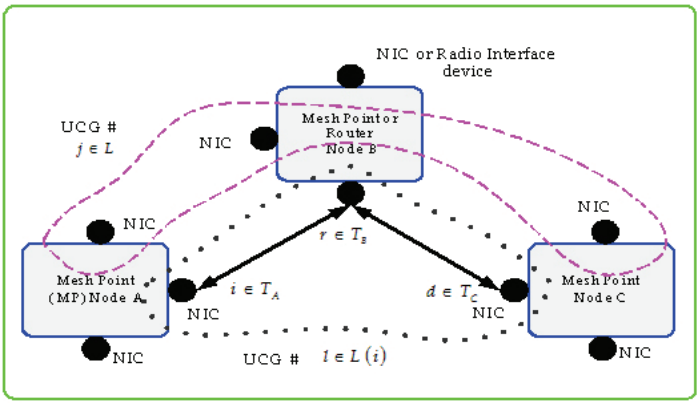

Fig. 1. MRMC multi-hop WBMN

Based on the UCG model depicted in Fig. 1, there exists an established logical topology, where some devices belonging to a certain UCG are *sources* of transmission, say $i \in T_A$ while certain devices act as 'voluntary' *relays*, say $r \in T_B$ to *destinations*, say $d \in T_C$. A sequence of connected *logical links* forms a *route* originating from source i. It should be noted that each asymmetrical physical link may be regarded as a multiple logical link due to the existence of multiple channels. Adjacent channels, actively transmitting packets simultaneously, cause adjacent channel interference (ACI) owing to their close proximity. The ACI can partly be reduced by dynamic channel assignment if implemented without run time overhead costs (Maheshwari et al., 2006). In this chapter, static channel assignment is assumed for every transmission time slot. Such an assumption is reasonable since the transmission power optimization is performed only by actively transmitting radios, to which channels have been assigned by the higher layers of the network protocol stack. It is pointless setting the time-scales for channel assignments to be greater than, or matching that, of power executions since the WMRs are assumed to be stationary. Furthermore, modern WMRs are built on

multiple cheap radio devices to simultaneously perform multi-point to multi-point (M2M) communication. Indeed, network accessing and backbone routing functionalities are effective while using separate radios. Each actively transmitting user acquires rights to the medium through a carrier sensed multiple access with collision avoidance (CSMA/CA) mechanism (Muqattash and Krunz, 2005). Such users divide their access time into a transmission power optimization mini-slot time and a data packet transmission mini-slot time interval. For analytical convenience, time slots will be normalized to integer units $t \in \{0,1,2,\ldots\}$ in the rest of the chapter.

3.2 Singularly-perturbed queue system

Suppose that N wireless links, each on a separate channel, emanate from a particular wireless MRMC node. Such links are assumed to contain N queues and consume N times energy associated with that node as illustrated by Fig. 2. It is noted that at the sender (and, respectively, the receiver), packets from a virtual MAC protocol layer termed as the PMMUP (respectively, multiple queues) are striped (respectively, resequenced) into multiple queues (respectively, PMMUP queues) (Olwal et al., 2009**b**; 2010**a**). Queues can be assumed to control the rates of the input packets to the finite-sized buffers. Such admission control mechanisms are activated if the energy residing in the node and the information from the upper layers are known a *priori*. Suppose that during a given time-slot, the application generates packets according to a Bernoulli process. Packets independently arrive at the multiple MAC and PHY queues with probability ϕ, where $\phi > 0$. Buffers' sizes of B packets are assumed. It should be considered that queues are initially nonempty and that new arriving packets are dropped when the queue is full; otherwise packets join the tail of the queue. The speed difference between the queue service rate and the energy level variations in the queue leads to the physical phenomenon called *perturbation*. Based on such perturbations, optimal transmission power is selected to send a serviced packet. It is noted that such a perturbation can conveniently be modelled by the Markov Chain process as follows:

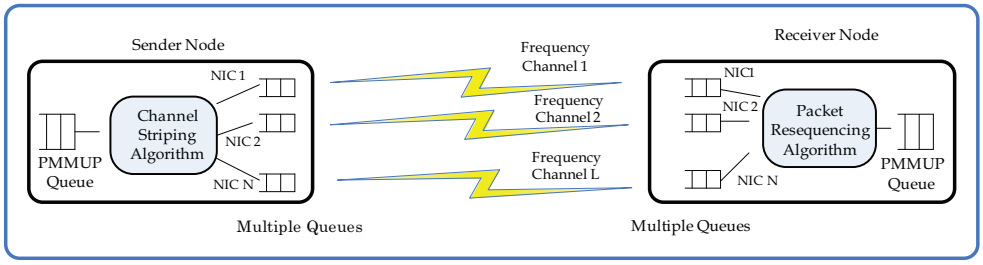

Fig. 2. Multiple queue system for a MRMC router-pair

Denote $i \in \mathrm{E}$, where $\mathrm{E} = \{1,2,\ldots,i,\ldots E\}$, as the energy level available for transmitting a packet over wireless medium by each NIC- pair (user). Denote φ_i, where $\varphi_i \in [0,1]$, as the probability of transmitting a packet with energy level i. The transition probability from energy state $X_n = i$ to state $X_{n+1} = j$ during the time transition $[n, n+1)$ is yielded by $\lambda_{ij} = \Pr(X_{n+1} = j \mid X_n = i)$. Let Λ, be the energy level transition matrix, where $\sum_{j=1}^{E} \lambda_{ij} = 1$ with the probability distribution denoted by $\vartheta = [\vartheta_1, \vartheta_2, \ldots, \vartheta_E]$ (El-Azouzi & Altman, 2003).

$$\Lambda = \begin{bmatrix} \lambda_{11} & \lambda_{12} & .. & \lambda_{1E} \\ \lambda_{21} & \lambda_{22} & .. & \lambda_{2E} \\ .. & .. & .. & .. \\ \lambda_{E1} & \lambda_{E2} & .. & \lambda_{EE} \end{bmatrix}, \tag{1}$$

It should be recalled that the power optimization phase requires information about the queue load and energy level dynamics. Denote $X(n) = \{X_n(i(n), j(n))\}$ as a two dimensional Markov chain sequence, where $i(n)$ and $j(n)$ are respectively the energy level available for packet transmission and the number of packets in the buffer at the nth time step. Let the packet arrival and the energy-charging/discharging process at each interface in time step $n+1$ be independent of the chain $X(n)$. Arrivals are assumed to occur at the end of the time step so that new arrivals cannot depart in the same time step that they arrive (Olwal et al., 2010**a**). Figure 3 depicts the two dimensional Markov chain evolution diagram with the transition probability matrix, $P_T(n)$, whose elements are $\lambda_{n,n+1}(i,j)$ for all $i = 1,2,\ldots,E$ and $j = 0,1,2,\ldots,B$. The notation, $\lambda_{n,n+1}(i,j)$ represents the transition probability of the *i*th energy level and the *j*th buffer level from state at *n* to state at *n+1*. In general, similar Markov chain representations can be assumed for other queues in a multi-queue system.

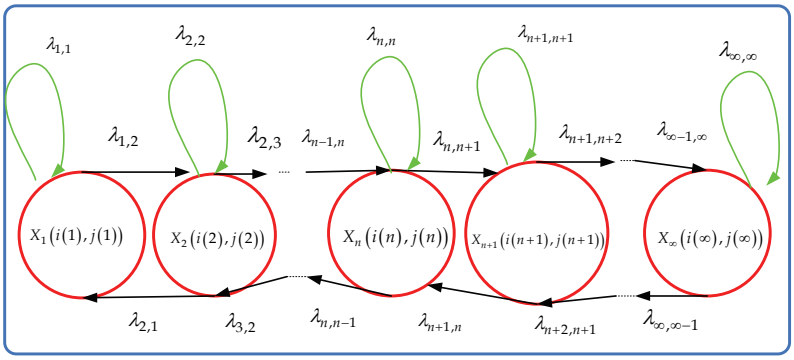

Fig. 3. Markov chain diagram

The transition probability $E(B+1)\times E(B+1)$ matrix of the Markov chain $X(n)$ is yielded by

$$P_T(n) = \begin{pmatrix} \mathbf{B}_0 & \mathbf{B}_1 & 0 & \cdots & \cdots & \cdots \\ \mathbf{A}_2 & \mathbf{A}_1 & \mathbf{A}_0 & 0 & \cdots & \cdots \\ 0 & \mathbf{A}_2 & \mathbf{A}_1 & \mathbf{A}_0 & 0 & \cdots \\ \vdots & \ddots & \ddots & \ddots & \ddots & \vdots \\ \vdots & \ddots & \ddots & \ddots & \mathbf{A}_1 & \mathbf{A}_0 \\ 0 & \cdots & \cdots & 0 & \mathbf{A}_2 & \mathbf{F}_1 \end{pmatrix} \begin{matrix} 0 \\ 1 \\ . \\ . \\ . \\ B \end{matrix}, \tag{2}$$

where $P_T(n)$ consists of $B+1$ block rows and $B+1$ block columns each of size $E\times E$. The matrices $\mathbf{B}_0$, $\mathbf{B}_1$, $\mathbf{A}_0$, $\mathbf{A}_1$, $\mathbf{A}_2$ and $\mathbf{F}_1$ are all $E\times E$ non-negative matrices denoted as $\mathbf{B}_0 = \bar{\phi}\Lambda$, $\mathbf{B}_1 = \phi\Lambda$, $\mathbf{A}_0 = \mathbf{diag}(\phi\bar{\varphi}_i,\ i = 1,\ldots,E)\Lambda$, $\mathbf{A}_1 = \mathbf{diag}(\phi\varphi_i + \bar{\phi}\bar{\varphi}_i,\ i = 1,\ldots,E)\Lambda$,

$\mathbf{A}_2 = \mathbf{diag}\left(\bar{\phi}\varphi_i \;\; i = 1, \ldots, E\right)\Lambda$ and $\mathbf{F}_1 = \mathbf{diag}\left(\phi\varphi_i + \bar{\varphi}_i \,,\; i = 1, \ldots, E\right)\Lambda$. Here $\bar{\phi} = 1 - \phi$ and $\bar{\varphi}_i = 1 - \varphi_i$ respectively denote the probability that no packet arrives in the queue and no packet is transmitted into the channel when the available energy level is i. If one assumes that the energy level transition matrix Λ is irreducible and aperiodic[1] and that $\phi > 0$, then the Markov chain $X(n)$ is aperiodic and contains a single ergodic class[2]. A unique row vector of steady state (or stationary) probability distribution can then be defined as $\pi(i,j) = \lim P_T\left(l(n)=i \,,\, b(n)=j\right),\; i = 1,2, \ldots, E \,,\;\; j = 0,1, \ldots, B$ and $\pi(i,j) \in \Re^{1 \times i(j+1)} \geq 0$. Let $\pi\left(i, j, \overset{n\to\infty}{\varepsilon_s}\right),\; i = 1, \ldots, i, \ldots, E \,,\;\; j = 0,1, \ldots j. \ldots, B$ be the probability distribution of the state of the available energy and the number of packets in the system in a steady state. Such a probability distribution $\pi(i,j,\varepsilon_s)$ can uniquely be determined by the following system

$$\pi(\varepsilon_s) P_T(\varepsilon_s) = \pi(\varepsilon_s) \,,\; \pi(\varepsilon_s)\mathbf{1} = 1 \,,\; \pi(\varepsilon_s) \geq 0 \,, \tag{3}$$

where ε_s denotes the *singular perturbation* factor depicting the speed ratio between energy and queue state evolutions. The first order Taylor series approximation of the perturbed Markov chain $X(n)$ transition matrix can be represented as $P_T(\varepsilon_s) = Q_0 + \varepsilon_s Q_1$, where Q_0 is the probability transition matrix of the unperturbed Markov chain corresponding to strong interactions while Q_1 is the generator corresponding to the weak interaction (El-Azouzi & Altman, 2003); that is,

$$Q_0 = \begin{pmatrix} \bar{\phi} I & \phi I & 0 & \cdots & \cdots & \cdots \\ \bar{\mathbf{A}}_2 & \bar{\mathbf{A}}_1 & \bar{\mathbf{A}}_0 & 0 & \cdots & \cdots \\ 0 & \bar{\mathbf{A}}_2 & \bar{\mathbf{A}}_1 & \bar{\mathbf{A}}_0 & 0 & \cdots \\ \vdots & \ddots & \ddots & \ddots & \ddots & \vdots \\ \vdots & \ddots & \ddots & \ddots & \ddots & \bar{\mathbf{A}}_0 \\ 0 & \cdots & \cdots & 0 & \bar{\mathbf{A}}_2 & \bar{\mathbf{F}}_1 \end{pmatrix}, \; Q_1 = \begin{pmatrix} \tilde{\mathbf{B}}_0 & \tilde{\mathbf{B}}_1 & 0 & \cdots & \cdots & \cdots \\ \tilde{\mathbf{A}}_2 & \tilde{\mathbf{A}}_1 & \tilde{\mathbf{A}}_0 & 0 & \cdots & \cdots \\ 0 & \tilde{\mathbf{A}}_2 & \tilde{\mathbf{A}}_1 & \tilde{\mathbf{A}}_0 & 0 & \vdots \\ \vdots & \ddots & \ddots & \ddots & \ddots & \vdots \\ \vdots & \ddots & \ddots & \ddots & \ddots & \tilde{\mathbf{A}}_0 \\ 0 & \cdots & \cdots & 0 & \tilde{\mathbf{A}}_2 & \tilde{\mathbf{F}}_1 \end{pmatrix}, \tag{4}$$

where

$\bar{\mathbf{A}}_2 = \mathbf{diag}\left(\bar{\phi}\varphi_i, i = 1, \ldots, E\right)$, $\bar{\mathbf{A}}_1 = \mathbf{diag}\left(\phi\varphi_i + \bar{\phi}\bar{\varphi}_i, i = 1, \ldots, E\right)$, $\bar{\mathbf{A}}_0 = \mathbf{diag}\left(\phi\bar{\varphi}_i, \; i = 1, \ldots, E\right)$,

$\bar{\mathbf{F}}_1 = \mathbf{diag}\left(\phi\varphi_i + \bar{\varphi}_i, \; i = 1, \ldots, E\right)$, $\tilde{\mathbf{B}}_0 = \bar{\phi}(\Lambda_1)$, $\tilde{\mathbf{B}}_1 = \phi(\Lambda_1)$, $\tilde{\mathbf{A}}_2 = \mathbf{diag}\left(\bar{\phi}\varphi_i, \; i = 1, \ldots E\right)\Lambda_1$,

$\tilde{\mathbf{A}}_1 = \mathbf{diag}\left(\phi\varphi_i\bar{\phi}\bar{\varphi}_i, \; i = 1, \ldots, E\right)\Lambda_1$, $\tilde{\mathbf{A}}_0 = \phi \; \mathbf{diag}\left(\phi\bar{\varphi}_i, i = 1, \ldots, E\right)\Lambda_1$ and

$\tilde{\mathbf{F}}_1 = \mathbf{diag}\left(\phi\varphi_i + \bar{\varphi}_i, \; i = 1, \ldots, E\right)\Lambda_1$.

Here,

$$\Lambda(\varepsilon_s) = I + \varepsilon_s \Lambda_1 \tag{5}$$

where Λ_1 is the generator matrix, representing an aggregated Markov chain $X(n)$.

The model in (2) to (5) leaves us with the perturbation problem under the assumption that an ergodic class exists (i.e., has exactly one closed communicating set of states), and Q_0

[1] A state evidences *aperiodic* behaviour if any return (returns) to the same state can occur at irregular multiple time steps.

[2] A Markov chain is called *ergodic* or *irreducible* if it is possible to go from every state to every other state.

contains E sub-chains (E ergodic class). The stationary probability $\pi(i,j,\varepsilon_s)$ from (3) of the perturbed Markov chain, therefore, takes a Taylor series expansion

$$\pi(i,j,\varepsilon_s) = \sum_{n=0}^{\infty} \pi^{(n)}(i,j)\varepsilon_s^n , \tag{6}$$

where ε_s^n is the nth order singularly-perturbed parameter. Denote the aggregate Markov chain probability distribution as $\bar{\vartheta} = \left[\bar{\vartheta}_1, \bar{\vartheta}_2, \ldots, \bar{\vartheta}_E\right]$. The unperturbed stationary probability is then yielded by $\pi^{(0)}(i,j) = \bar{\vartheta}_i \nu_{\zeta_i}(j)$ where ν_{ζ_i} is the probability distribution of the recurrent class ζ_i, i.e., $\sum_{j=0}^{B} \zeta_i(j) = 1$.

3.3 Weakly-coupled multi-channel system

Theoretically, simultaneous transmitting links on different orthogonal channels are expected not to conflict with each other. However, wireless links emanating from the same node of a multi-radio system do conflict with each other owing to their close vicinity. The radiated power coupling across multiple channels results in the following: loss in signal strength owing to inter-channel interference; hence packet losses over multi-channel wireless links. Such losses lead to packet retransmissions and hence queue instabilities along a link(s). Retransmissions also cause high energy consumption in the network. Highly energy-depleted networks result in poor network connectivity. Therefore, one can model the wireless cross-channel interference (interaction) as a weakly-coupled system (Olwal et al., 2010**a**). Each transmitter-receiver pair (user) operating on a particular channel (i.e., UCG) adjusts its transmission power dynamically, based on a sufficiently small positive parameter denoted as ε_w.

As an illustration, let us consider a two-dimensional node placement consisting of two co-located orthogonal wireless channels labelled i and j with simultaneous radial transmissions as depicted in Fig. 4. The coupled region is denoted by surface area A_ε. Since power coupling is considered, the weak coupling factor can be derived as a function of the region or surface A_ε, i.e., $O(d_{ij}^2)$, where d_{ij} is the distance between point i and j. From the geometry of Fig. 4, it is easy to demonstrate that the weak coupling parameter yields,

$$\varepsilon_{ij} = \frac{\mathrm{A}_{\varepsilon i}}{\mathrm{A}_\varepsilon} = \frac{d_i^2\left[\theta_i - \frac{\sin\theta_i}{\sqrt{2}}\right]}{d_i^2\left[\theta_i - \frac{\sin\theta_i}{\sqrt{2}}\right] + d_j^2\left[\theta_j - \frac{\sin\theta_j}{\sqrt{2}}\right]}, \varepsilon_{ji} = \frac{\mathrm{A}_{\varepsilon j}}{\mathrm{A}_\varepsilon} = \frac{d_j^2\left[\theta_j - \frac{\sin\theta_j}{\sqrt{2}}\right]}{d_i^2\left[\theta_i - \frac{\sin\theta_i}{\sqrt{2}}\right] + d_j^2\left[\theta_j - \frac{\sin\theta_j}{\sqrt{2}}\right]} . \tag{7}$$

Thus, the weakly-coupled scalar is generally a function of the square of the transmission radii (d_i and d_j) and the coupling-sector angles (θ_i and θ_j). The weak coupling parameter is bounded by $0 < \varepsilon_{ij} = \varepsilon_w < 1$. The sectored angle has a bound, $0 \le \theta \le 2\pi$ in radians.

It should be noted that both the singular perturbation and weak coupling models at the multiple MACs and radio interfaces are coordinated by the virtual MAC protocol at the Link Layer. The motivation is to conceal the complexity of multiple lower layers from the higher layers of the protocol stack, without additional hardware modifications.

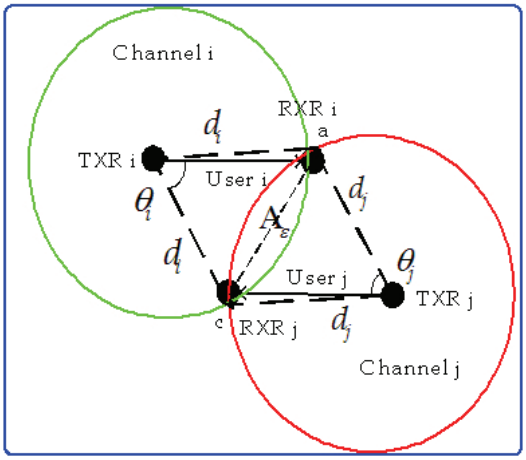

Fig. 4. A weakly-coupled wireless channel dual system of two simultaneously co-located transmitting users *i* and *j* described by infinitesimally small radiating points TXR *i* and RXR *i* pair, and TXR *j* and RXR *j* pair, respectively.

3.3 Optimal problem formulation

For *N* users at each WMR, the SPWC large-scale linear dynamic system is written as (Gajic & Shen, 1993; Mukaidani, 2009; Sagara et al., 2008),

$$\mathbf{x}_i(t+1) = \mathbf{A}_{ii}(\varepsilon)\mathbf{x}_i(t) + \mathbf{B}_{ii}(\varepsilon)\mathbf{u}_i(t) + \mathbf{W}_{ii}(\varepsilon)\mathbf{w}_i(t) + \sum_{\substack{j=1 \\ j\neq i}}^{N} \varepsilon_{ij}\mathbf{A}_{ij}\mathbf{x}_j(t) + \sum_{\substack{j=1 \\ j\neq i}}^{N} \varepsilon_{ij}\mathbf{B}_{ij}\mathbf{u}_j(t) + \sum_{\substack{j=1 \\ j\neq i}}^{N} \varepsilon_{ij}\mathbf{W}_{ij}\mathbf{w}_j(t),$$

$$\mathbf{y}_i(t) = \mathbf{C}_{ii}(\varepsilon)\mathbf{x}_i(t) + \sum_{\substack{j=1 \\ j\neq i}}^{N} \varepsilon_{ij}\mathbf{C}_{ij}\mathbf{x}_j(t) + \mathbf{v}_i(t),\ \mathbf{x}_i(0) = \mathbf{x}_i^0,\ i = 1,\ldots,N, \tag{8}$$

where $\mathbf{x}_i \in \Re^{n_i}$ represents the state vector of the *i*th user, $\mathbf{u}_i \in \Re^{m_i}$ is the control input of the *i*th user, $\mathbf{w}_i \in \Re^{q_i}$ represents the Gaussian distributed zero mean disturbance noise vector to the *i*th user, $\mathbf{y}_i \in \Re^{l_i}$ represents the observed output and $\mathbf{v}_i \in \Re^{l_i}$ are the Gaussian distributed zero mean measurement noise vectors. The white noise processes $\mathbf{w}_i \in \Re^{q_i}$ and $\mathbf{v}_i \in \Re^{l_i}$ are independent and mutually uncorrelated with intensities $\Theta_{\mathbf{w}} > 0$ and $\Theta_{\mathbf{v}} > 0$, respectively. The system matrices **A**, **B**, **C** and **W** are defined in the same way as discussed in our recent invesitigation (Olwal et al., 2009**b**).

Let the partitioned matrices for the wireless MRMC node pair with the weak-coupling to the singular-perturbation ratio $0 < \varepsilon = \frac{\varepsilon_w}{\varepsilon_s} < \infty$, be defined as follows:

$$\mathbf{A}_{\varepsilon}=\begin{bmatrix}\mathbf{A}_{11}(\varepsilon) & \varepsilon_{12}\mathbf{A}_{12} & \dots & \varepsilon_{1N}\mathbf{A}_{1N}\\ \varepsilon_{21}\mathbf{A}_{21} & \mathbf{A}_{22}(\varepsilon) & \dots & \varepsilon_{2N}\mathbf{A}_{2N}\\ . & . & . & .\\ \varepsilon_{N1}\mathbf{A}_{N1} & \varepsilon_{N2}\mathbf{A}_{N2} & \dots & \mathbf{A}_{NN}(\varepsilon)\end{bmatrix},\ \mathbf{B}_{i\varepsilon}=\begin{bmatrix}\varepsilon^{1-\delta_{1i}}\mathbf{B}_{1i}\\ \varepsilon^{1-\delta_{2i}}\mathbf{B}_{2i}\\ .\\ \varepsilon^{1-\delta_{Ni}}\mathbf{B}_{Ni}\end{bmatrix},\ \delta_{ij}=\begin{cases}0\,(i\neq j)\\ 1\,(i=j)\end{cases},$$

$$\mathbf{W}_{\varepsilon}=\begin{bmatrix}\mathbf{W}_{11}(\varepsilon) & \varepsilon_{12}\mathbf{W}_{12} & \dots & \varepsilon_{1N}\mathbf{W}_{1N}\\ \varepsilon_{21}\mathbf{W}_{21} & \mathbf{W}_{22}(\varepsilon) & \dots & \varepsilon_{2N}\mathbf{W}_{2N}\\ . & . & . & .\\ \varepsilon_{N1}\mathbf{W}_{N1} & \varepsilon_{N2}\mathbf{W}_{N2} & \dots & \mathbf{W}_{NN}(\varepsilon)\end{bmatrix},\ \mathbf{C}_{\varepsilon}=\begin{bmatrix}\mathbf{C}_{11}(\varepsilon) & \varepsilon_{12}\mathbf{C}_{12} & \dots & \varepsilon_{1N}\mathbf{C}_{1N}\\ \varepsilon_{21}\mathbf{C}_{21} & \mathbf{C}_{22}(\varepsilon) & \dots & \varepsilon_{2N}\mathbf{C}_{2N}\\ . & . & . & .\\ \varepsilon_{N1}\mathbf{C}_{N1} & \varepsilon_{N2}\mathbf{C}_{N2} & \dots & \mathbf{C}_{NN}(\varepsilon)\end{bmatrix}. \quad (9)$$

Each strategy user is faced with the *minimization problem* along trajectories of a linear dynamic system in (8),

$$J_i\left(u_1,\dots,u_N,\mathbf{w},\mathbf{x}(0)\right)=\frac{1}{2}\mathrm{E}\left\{\lim_{t\to\infty}\frac{1}{t}\sum_{\tau=0}^{t-1}\begin{bmatrix}\mathbf{z}^T(\tau)\mathbf{z}(\tau)+\mathbf{u}_i^T(\tau)\mathbf{R}_{ii}\mathbf{u}_i(\tau)\\ +\sum_{\substack{j=1\\ j\neq i}}^{N}\varepsilon_{ij}\mathbf{u}_j^T(\tau)\mathbf{R}_{ij}\mathbf{u}_j(\tau)-\mathbf{w}^T(t)\Theta_{\mathbf{w}i\varepsilon}\mathbf{w}(t)\end{bmatrix}\right\}, \quad (10)$$

where $\mathbf{z}\in\Re^{s}$ is the controlled output with dimension equal to s, given by (Gajic & Shen, 1993),

$$\mathbf{z}_i(t)=\mathbf{D}_{ii}(\varepsilon)\mathbf{x}_i(t)+\sum_{\substack{j=1\\ j\neq i}}^{N}\varepsilon_{ij}\mathbf{D}_{ij}\mathbf{x}_j(t), \quad (11)$$

with

$$\mathbf{D}_{\varepsilon}=\begin{bmatrix}\mathbf{D}_{11}(\varepsilon) & \varepsilon_{12}\mathbf{D}_{12} & \dots & \varepsilon_{1N}\mathbf{D}_{1N}\\ \varepsilon_{21}\mathbf{D}_{21} & \mathbf{D}_{22}(\varepsilon) & \dots & \varepsilon_{2N}\mathbf{D}_{2N}\\ . & . & . & .\\ \varepsilon_{N1}\mathbf{D}_{N1} & \varepsilon_{N2}\mathbf{D}_{N2} & \dots & \mathbf{D}_{NN}(\varepsilon)\end{bmatrix},\ \mathbf{R}_{ii}=\mathbf{R}_{ii}^T>0\in\Re^{m_i\times m_i},\ \mathbf{R}_{ij}=\mathbf{R}_{ij}^T\geq 0\in\Re^{m_j\times m_j},$$

$$\in\Re^{\bar{n}\times\bar{n}}$$

$$\Theta_{\mathbf{w}i\varepsilon}=\mathbf{block\ diag}\left(\varepsilon_{i1}^{-(1-\delta_{i1})}\Theta_{\mathbf{w}i1}\dots\varepsilon_{iN}^{-(1-\delta_{iN})}\Theta_{\mathbf{w}iN}\right)\geq 0\in\Re^{\bar{q}\times\bar{q}},\ i,\ j=1,\dots,N\ .$$

4. Transmission power management scheme

In order to manage SPWC optimal control problems at the complex MAC and PHY layers, a *singularly-perturbed weakly-coupled power selection multi-radio multi-channel unification protocol* (SPWC-PMMUP) is suggested. The SPWC-PMMUP firmware architecture is depicted in Fig. 5. The design rationale of the firmware is to perform an energy-efficient transmission power management (TPM) in a multi-radio system with minimal change to the existing standard compliant wireless technologies. Such TPM schemes may adapt even to a heterogeneous multi-radio system (i.e., each node has a different number of radios) experiencing singular

perturbations. The SPWC-PMMUP coordinates the optimal TPM executions in UCGs. The key attributes are that the SPWC-PMMUP scheme minimizes the impacts of: (i) queue perturbations, arising between energy and packet service variations, and (ii) cross-channel interference problems owing to the violation of orthogonality of multiple channels by wireless fading. The proposed TPM scheme is discussed in the following sections: 4.1 and 4.2.

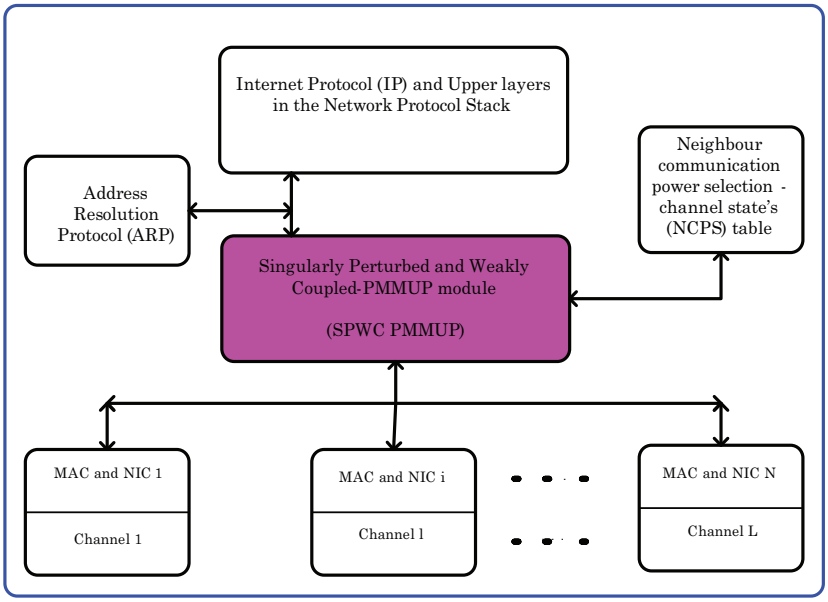

Fig. 5. Singularly-perturbed weakly-coupled PMMUP architecture

4.1 Timing phase structure

The SPWC-PMMUP contains L parallel channel sets with the *virtual* timing structure shown in Fig. 6. Channel access times are divided into identical time-slots. There are three phases in each time-slot after slot synchronization. Phase I serves as the channel probing or Link State Information (LSI) estimation phase. Phase II serves as the *Ad Hoc traffic indication message* (ATIM) window which is on when power optimization occurs. Nodes stay awake and exchange an ATIM (indicating such nodes' intention to send the queue data traffic) message with their neighbours (Wang et al., 2006). Based on the exchanged ATIM, each user performs an optimal transmission power selection (adaptation) for eventual data exchange. Phase III serves as the data exchange phase over power controlled multiple channels.

Phase I: In order for each user to estimate the number of active links in the same UCG, Phase I is divided into M mini-slots. Each mini-slot lasts a duration of channel probing time T_{cp}, which is set to be large enough for judging whether the channel is busy or not. If a link has traffic in the current time-slot, it may randomly select one probe mini-slot and transmit a busy signal. By counting the busy mini-slots, all nodes can estimate how many links intend to advertise traffic at the end of Phase I. Additionally, the SPWC-PMMUP estimates: the inter channel interference (i.e., weak coupling powers), the intra-UCG interference (i.e., the strong coupling powers), the queue perturbation and the LSI addressed in (Olwal et al.,

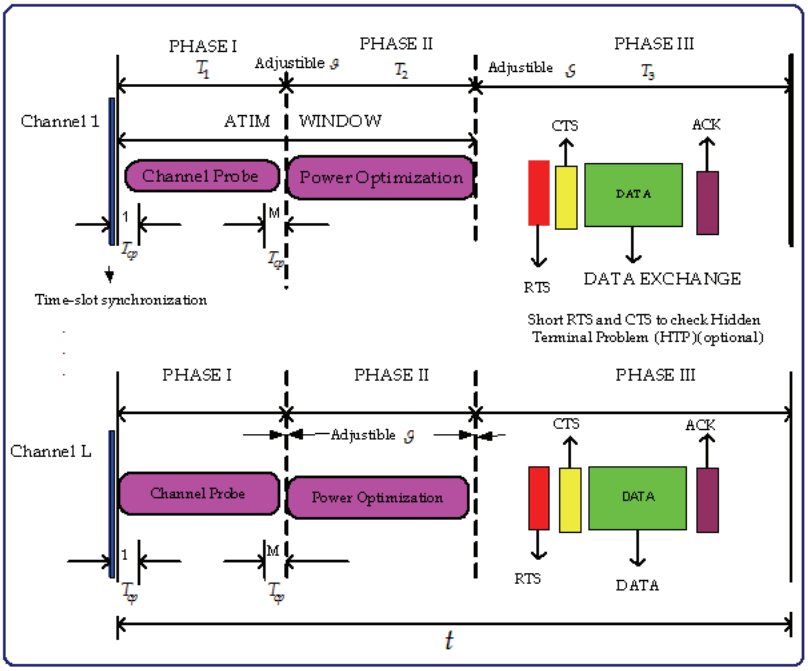

Fig. 6. The virtual SPWC-PMMUP timing structure

2009**a**). It should be noted that the number of links intending to advertise traffic, if not zero, could be greater than the observed number of busy mini-slots. This occurs because there might be at least one link intending to advertise traffic during the same busy mini-slot.

Denote the number of neighbouring links in the same UCG intending to advertise traffic at the end of Phase I as n. Given M and n, the probability that the number of observed busy mini-slots equals m, is calculated by

$$P_r(M,n,m) = \frac{\binom{M}{m}\binom{n-1}{m-1}}{\binom{n+M-1}{M-1}} \tag{12}$$

Let n remain the same for the duration of each time-slot t. Denote the estimate of the number of active links as $\hat{n}(t)$ and the probability mass function (PMF) that the number of busy mini-slots observed in the previous time-slot equals k as $f_k(t)$. Denote $m(t)$ as the number of the current busy mini-slots. The estimate $\hat{n}(t)$ is then derived from the estimation error process as,

$$\hat{n}(t) = \arg\min_{n \geq m(t)} \left\{ \sum_{k=m(t)}^{n} P_r(M,n,k) - \sum_{k=m(t)}^{n} f_k(t) \right\}, \tag{13}$$

where $f_k(t)$ from one time-slot to other is updated as

$$f_k(t) = \begin{cases} (1-\alpha(t)) f_k(t-1), & k \neq m(t) \\ (1-\alpha(t)) f_m(t-1) + \alpha(t), & k = m(t) \end{cases}, \quad (14)$$

and $\alpha(t), (0 < \alpha(t) < 1)$ is the PMF update step size, which needs to be chosen appropriately to balance the convergence speed and the stability. Of course, selecting a large value of M when Phase I is adjusted to be narrower will imply short T_{cp} periods and negligible delay during the probing phase. Short channel probing phase time allows time for large actual data payload exchange, consequently improving network capacity.

Phase II: In this phase, the TPM problem and solution are implemented. Suppose the number of busy mini-slots is non-zero; then the SPWC-PMMUP module performs a power optimization following the $p-$ persistent algorithm or back-off algorithm (Wang et al., 2006). Otherwise, the transmission power optimization depends on the queue status only (i.e., the evaluation of the singular perturbation of the queue system). The time duration of the power optimization is denoted as T_2 and the minimal duration to complete power optimization as a function of the number of participating users in a p-persistent CSMA, is denoted as $T_{succ}(n, p^*)$. The transmission power optimization time allocation T_2 is then adjusted according to

$$T_2 = \min\left\{T_2^{\max}, \vartheta \sum_{n=1}^{\hat{n}} T_{succ}(n, p^*)\right\}, \quad (15)$$

where $T_2^{\max}$ is the power allocation upper bound time, ϑ is the power allocation time adjusting parameter and $\hat{n}$ is the estimated number of actively interfering neighbour links in the same UCG. The steady state medium access probability p in terms of the minimal average service time can be computed as (Wang et al., 2006),

$$p^* = \arg\min_{0<p<1}\left\{T_{succ}(n, p)\right\}. \quad (16)$$

It should be noted that due to energy conservation, T_1 and T_2 should be short enough and the optimal p^* can be obtained from a look up table rather than from online computation. The TPM solution is then furnished according to section 4.2.

Phase III: Data is exchanged by NICs over parallel multiple non-overlapping channels within a time period of T_3. The RTS/CTS are exchanged at the probe power level which is sufficient in order to resolve collisions due to hidden terminal nodes. Furthermore, the optimal medium access probability p^* resolves RTS/CTS collisions. After sending data traffic to the target receiver, each node may determine the achievable throughput according to,

$$Th_r(t) = \frac{\tilde{L}}{t}\left\{\sum_i \left\{ P_i^{swp}(\vec{n}_{swp}, \vec{p}_{swp}, T_2) \times \sum_{l=1}^{L} \sum_j j\, P_j^{l,data}(\vec{n}_{l,data}, \vec{p}_{l,data}, T_3)\right\}\right\}. \quad (17)$$

Here, $\tilde{L}$ is the application/data packet length and t is the length of one virtual time-slot which equals $T_1 + T_2 + T_3$. Denote $P_i^{swp}(\vec{n}_{swp}, \vec{p}_{swp}, T_2)$ as the SPWC based probability that i actively interfering links successfully exchange ATIM in Phase II, given the number of links intending to advertise traffic as, $\vec{n}_{swp}$ and the medium access probability sequence as, $\vec{p}_{swp}$

during time T_2 period. Denote $P_i^{l,data}\left(\vec{n}_{l,data},\vec{p}_{l,data},T_3\right)$ as the probability that i data packets are successfully exchanged on channel l in Phase III, given the number sequence $\vec{n}_{l,data}$ and the medium access probability sequence as $\vec{p}_{l,data}$ during time T_3 period. The computations of such probabilities have been provided in (Li et al., 2009). If several transmissions are executed, then the average throughput performance can be evaluated. The energy efficiency in joules per successfully transmitted packets then becomes

$$E_{eff}=\frac{optimal\ transmission\ power\ per\ node\left(watts\right)}{average\ throughput\ per\ node\left(packets/\mathrm{s}\right)}. \tag{18}$$

It should be noted that a high throughput implies a low energy-efficiency for a given optimal power level, because of the high data payload needed to successfully reach the intended receiver within a given time slot. The use of an optimal power level is expected to yield a better spectrum efficiency and throughput measurement balance.

4.2 Nash strategies

The optimal solution to the given problem (10) with the conflict of interest and simultaneous decision making leads to the so called Nash strategies (Gajic & Shen, 1993) $\mathbf{u}_1^*,\ldots,\mathbf{u}_i^*,\ldots,\mathbf{u}_N^*$ satisfying

$$J_i\left(\mathbf{u}_1^*,\ldots,\mathbf{u}_i^*,\ldots,\mathbf{u}_N^*,\mathbf{x}(0)\right)$$

$$\le J_i\left(\mathbf{u}_1^*,\ldots,\mathbf{u}_i,\ldots,\mathbf{u}_N^*,\mathbf{x}(0)\right),\ \mathbf{u}_i^*\ne\mathbf{u}_i,\ i=1,\ldots,N. \tag{19}$$

Assumption 1: *Each* ith *user has optimal closed-loop Nash strategies yielded by*

$$\mathbf{u}_i^*(t)=-\mathbf{F}_{i\varepsilon}^*\mathbf{x}(t),\quad i=1,\ldots,N. \tag{20}$$

Here, the decoupled $\mathbf{F}_{i\varepsilon}^*$ is the regulator feedback gain with singular-perturbation and weak-coupling components defined as

$$\mathbf{F}_{i\varepsilon}=\left[\varepsilon^{1-\delta_{1i}}\mathbf{F}_{1i}\ \varepsilon^{1-\delta_{2i}}\mathbf{F}_{2i}\ \ldots\ \varepsilon^{1-\delta_{Ni}}\mathbf{F}_{Ni}\right]\in\Re^{\bar{n}}, \tag{21}$$

with $\bar{n}=\sum_{i=1}^{N}n_i$, n_i is the size of the vector $\mathbf{x}_i$ and $\delta_{ij}=\begin{cases}0\ (i\ne j)\\1\ (i=j)\end{cases}$.

Define the N-tuple discrete in time Nash strategies by

$$\mathbf{u}_i^*(t)=-\mathbf{F}_{i\varepsilon}^*\mathbf{x}(t)=-\left(\mathbf{R}_{ii}+\mathbf{B}_{i\varepsilon}^T\mathbf{P}_{i\varepsilon}\mathbf{B}_{i\varepsilon}\right)^{-1}\mathbf{B}_{i\varepsilon}^T\mathbf{P}_{i\varepsilon}\mathbf{A}_\varepsilon\mathbf{x}(t),\quad i=1,\ldots,N, \tag{22}$$

where $\left(\mathbf{F}_{1\varepsilon}^*,\ldots,\mathbf{F}_{N\varepsilon}^*\right)\in F_N$ and N-tuple $\mathbf{u}_i^*(t)$, form a soft constrained Nash Equilibrium represented as

$$J_i\left(\mathbf{F}_{1\varepsilon}^*\mathbf{x},\ldots,\mathbf{F}_{N\varepsilon}^*\mathbf{x},\mathbf{x}(0)\right)=\mathbf{x}(0)^T\mathbf{P}_{i\varepsilon}\mathbf{x}(0). \tag{23}$$

Here, the decoupled $\mathbf{P}_{i\varepsilon}$ is a positive semi-definite stabilizing solution of the discrete-time algebraic regulator Riccati equation (DARRE) with the following structure:

$$\mathbf{P}_{i\varepsilon} = \mathbf{P}_{i\varepsilon}^T = \begin{bmatrix} \varepsilon_{i1}^{1-\delta_{i1}}\mathbf{P}_{i1} & \varepsilon_{i2}\mathbf{P}_{i12} & . & \varepsilon_{iN}\mathbf{P}_{i1N} \\ \varepsilon_{i2}\mathbf{P}_{i12}^T & \varepsilon_{i2}^{1-\delta_{i2}}\mathbf{P}_{i2} & . & \varepsilon_{iN}\mathbf{P}_{i2N} \\ . & . & . & . \\ \varepsilon_{iN}\mathbf{P}_{i1N}^T & \varepsilon_{iN}\mathbf{P}_{i2N}^T & . & \varepsilon^{1-\delta_{iN}}\mathbf{P}_{iN} \end{bmatrix}, \quad \in \Re^{\bar{n}\times\bar{n}} \tag{24}$$

where the DARRE is given by

$$\mathbf{P}_\varepsilon = \mathbf{D}_\varepsilon^T\mathbf{D}_\varepsilon + \mathbf{A}_\varepsilon^T\mathbf{P}_\varepsilon\mathbf{A}_\varepsilon - \mathbf{A}_\varepsilon^T\mathbf{P}_\varepsilon\mathbf{B}_\varepsilon\left(\mathbf{R}_\varepsilon + \mathbf{B}_\varepsilon^T\mathbf{P}_\varepsilon\mathbf{B}_\varepsilon\right)^{-1}\mathbf{B}_\varepsilon^T\mathbf{P}_\varepsilon\mathbf{A}_\varepsilon, \tag{25}$$

with

$$\mathbf{R} = \mathbf{diag}\left(\mathbf{R}_1 \ldots \mathbf{R}_N\right), \quad \mathbf{D}_\varepsilon = \begin{bmatrix} \mathbf{D}_{11}(\varepsilon) & \varepsilon_{12}\mathbf{D}_{12} & \ldots & \varepsilon_{1N}\mathbf{D}_{1N} \\ \varepsilon_{21}\mathbf{D}_{21} & \mathbf{D}_{22}(\varepsilon) & \ldots & \varepsilon_{2N}\mathbf{D}_{2N} \\ . & . & . & . \\ \varepsilon_{N1}\mathbf{D}_{N1} & \varepsilon_{N2}\mathbf{D}_{N2} & \ldots & \mathbf{D}_{NN}(\varepsilon) \end{bmatrix}. \quad \in \Re^{\bar{n}\times\bar{n}}$$

It should be noted that the inversion of the partitioned matrices $\mathbf{R}_\varepsilon + \mathbf{B}_\varepsilon^T\mathbf{P}_\varepsilon\mathbf{B}_\varepsilon$ in (25) will produce numerous terms and cause the DARRE approach to be computationally very involved, even though one is faced with the reduced-order numerical problem (Gajic & Shen, 1993). This problem is resolved by using bilinear transformation to transform the discrete-time Riccati equations (DARRE) into the continuous-time algebraic Riccati equation (CARRE) with equivalent co-relation.

The differential game Riccati matrices $\mathbf{P}_{i\varepsilon}$ satisfy the singularly-perturbed and weakly-coupled, continuous in time, algebraic Regulator Riccati equation (SWARREs) (Gajic & Shen, 1993; Sagara et al., 2008) which is given below,

$$\Omega_i\left(\mathbf{P}_{1\varepsilon}, \ldots, \mathbf{P}_{i\varepsilon}, \ldots, \mathbf{P}_{N\varepsilon}\right) = \mathbf{P}_{i\varepsilon}\left(\mathbf{A}_\varepsilon - \sum_{\substack{j=1 \\ j\neq i}}^{N}\mathbf{S}_{j\varepsilon}\mathbf{P}_{j\varepsilon}\right) + \left(\mathbf{A}_\varepsilon - \sum_{\substack{j=1 \\ j\neq i}}^{N}\mathbf{S}_{j\varepsilon}\mathbf{P}_{j\varepsilon}\right)^T\mathbf{P}_{i\varepsilon}$$

$$-\mathbf{P}_{i\varepsilon}\mathbf{S}_{i\varepsilon}\mathbf{P}_{i\varepsilon} + \sum_{\substack{j=1 \\ j\neq i}}^{N}\varepsilon_{ij}\mathbf{P}_{j\varepsilon}\mathbf{S}_{ij\varepsilon}\mathbf{P}_{j\varepsilon} + \mathbf{P}_{i\varepsilon}\mathrm{M}_{i\varepsilon}\mathbf{P}_{i\varepsilon} + \mathbf{D}^T{}_{i\varepsilon}\mathbf{D}_{i\varepsilon} = \mathbf{0}, \tag{26}$$

where

$$\mathbf{S}_{i\varepsilon} = \mathbf{B}_{i\varepsilon}\mathbf{R}_{ii}^{-1}\mathbf{B}_{i\varepsilon}^T, i = 1, \ldots, N. \quad \mathbf{S}_{ij} = \mathbf{B}_{j\varepsilon}\mathbf{R}_{jj}^{-1}\mathbf{R}_{ij}\mathbf{R}_{jj}^{-1}\mathbf{B}_{j\varepsilon}^T, \ i = 1, \ldots, N.$$

$$\mathrm{M}_{i\varepsilon} = \mathbf{W}_\varepsilon\Theta_{\mathbf{w}i\varepsilon}^{-1}\mathbf{W}_\varepsilon, \ i = 1, \ldots, N.$$

By substituting the partitioned matrices of $\mathbf{A}_{\varepsilon}$, $\mathbf{S}_{i\varepsilon}$, $\mathbf{S}_{ij\varepsilon}$, $\mathrm{M}_{i\varepsilon}$, $\mathbf{D}_{i\varepsilon}$, and $\mathbf{P}_{i\varepsilon}$ into SWARRE (26), and by letting $\varepsilon_w = 0$ and any $\varepsilon_s \neq 0$, then simplifying the SWARRE (26), the following reduced order (auxiliary) algebraic Riccati equation is obtained,

$$\mathbf{P}_{ii}\mathbf{A}_{ii} + \mathbf{A}_{ii}^{T}\mathbf{P}_{ii} - \mathbf{P}_{ii}\left(\mathbf{S}_{ii} - \mathrm{M}_{ii}\right)\mathbf{P}_{ii} + \mathbf{D}_{ii}^{T}\mathbf{D}_{ii} = 0\,, \tag{27}$$

where $\mathbf{S}_{ii} = \mathbf{B}_{ii}\mathbf{R}_{ii}^{-1}\mathbf{B}_{ii}^{T}$ and $\mathrm{M}_{ii} = \mathbf{W}_{ii}\Theta_{ii}^{-1}\mathbf{W}_{ii}^{T}$, and $\mathbf{P}_{ii}$, $i = 1, \ldots, N$ is the 0-order approximation of $\mathbf{P}_{i\varepsilon}$ when the weakly-coupled component is set to zero, i.e., $\varepsilon_w = 0$. It should be noted that a unique positive semi-definite optimal solution $\mathbf{P}_{i\varepsilon}^{*}$ exists if the following assumptions are taken into account (Mukaidani, 2009).

Assumption 2: *The triples* $\mathbf{A}_{ii}$, $\mathbf{B}_{ii}$ *and* $\mathbf{D}_{ii}$, $i = 1, \ldots, N$, *are stabilizable and detectable.*

Assumption 3: *The auxiliary (27) has a positive semidefinite stabilizing solution such that* $\tilde{\mathbf{A}} = \mathbf{A}_{ii} - \mathbf{S}_{ii}\mathbf{P}_{ii}$ *is stable.*

4.3 Analysis of SPWC-PMMUP optimality

Lemma 1: *Under assumption 3 there exists a small constant* ∂^{*} *such that for all* $\tilde{\varepsilon}(t) \in \left(0, \partial^{*}\right)$, *SWARRE admits a positive definite solution* $\mathbf{P}_{i\varepsilon}^{*}$ *represented as*

$$\mathbf{P}_{i\varepsilon} = \mathbf{P}_{i\varepsilon}^{*} = \mathbf{P}_{i} + O\left(\varepsilon(t)\right),\ i = 1, \ldots, N \quad \text{and} \quad \tilde{\varepsilon}(t) = \left|\sqrt{\varepsilon_w \varepsilon_s}\right|,$$

$$= \textbf{block diag}\left(0 \ldots \mathbf{P}_{ii} \ldots 0\right) + O\left(\tilde{\varepsilon}(t)\right). \tag{28}$$

Proof: This can be achieved by demonstrating that the Jacobian of SWARRE is non-singular at $\tilde{\varepsilon}(t) = 0$ and its neighbourhood, i.e., $\varepsilon(t) \to +0$. Differentiating the function $\Omega_i\left(\tilde{\varepsilon}(t), \mathbf{P}_{1\varepsilon}, \ldots, \mathbf{P}_{N\varepsilon}\right)$ with respect to the decoupled matrix $\mathbf{P}_{i\varepsilon}$ produces,

$$\mathbf{J}_{ii} = \frac{\partial}{\partial\, vec\, \mathbf{P}_{i\varepsilon}}\, vec\, \Omega_i\left(\tilde{\varepsilon}(t), \mathbf{P}_{1\varepsilon}, \ldots, \mathbf{P}_{N\varepsilon}\right)^{T} = \Delta_{ii}^{T} \otimes I_{n_i} + I_{n_i} \otimes \Delta_{ii}^{T}.$$

$$\mathbf{J}_{ij} = \frac{\partial}{\partial\, vec\ P_{ij}}\, vec\, \Omega_i\left(\tilde{\varepsilon}(t), \mathbf{P}_{1\varepsilon}, \ldots, \mathbf{P}_{N\varepsilon}\right)^{T},$$

$$= -\left(\mathbf{S}_{j\varepsilon}\mathbf{P}_{i\varepsilon} - \tilde{\varepsilon}_{ij}\mathbf{S}_{ij\varepsilon}\mathbf{P}_{j\varepsilon}\right)^{T} \otimes I_{n_i} - I_{n_i} \otimes \left(\mathbf{S}_{j\varepsilon}\mathbf{P}_{i\varepsilon} - \tilde{\varepsilon}_{ij}\mathbf{S}_{ij\varepsilon}\mathbf{P}_{j\varepsilon}\right)^{T}, \tag{29}$$

where $i \neq j$, $j = 1, \ldots, N$ and $\Delta = \mathbf{A}_{\varepsilon} - \sum_{\substack{j=1 \\ i \neq j}}^{N} \mathbf{S}_{j\varepsilon}\mathbf{P}_{j\varepsilon} + \mathrm{M}_{i\varepsilon}\mathbf{P}_{i\varepsilon}$.

Exploiting the fact that $\mathbf{S}_{j\varepsilon}\mathbf{P}_{i\varepsilon} = O(\tilde{\varepsilon}(t))$ for $i \neq j$, the Jacobian of SWARRE with $\tilde{\varepsilon}(t) \to +0$ can be verified as

$$\hat{\mathbf{J}} = \textbf{block diag}\left(\Delta_{11} \ldots \Delta_{NN}\right),\ \mathbf{J} = \textbf{block diag}\left(\hat{\mathbf{J}} \ldots \hat{\mathbf{J}}\right).$$

Since the determinant of $\Delta_{ii} = \mathbf{A}_{ii} - \mathbf{S}_{ii}\mathbf{P}_{ii} + \mathbf{M}_{ii}\mathbf{P}_{ii}$ with $\tilde{\varepsilon}(t) = 0$ is non-zero by following assumption 3 for all $i = 1, \ldots, N$, thus $\det \mathbf{J} \neq 0$ i.e., $\mathbf{J}$ is non-singular for $\tilde{\varepsilon}(t) = 0$. As a consequence of the implicit function theorem, $\mathbf{P}_{ii}$ is a positive definite matrix at $\tilde{\varepsilon}(t) = 0$ and for sufficiently small parameters $\tilde{\varepsilon}(t) \in (0, \partial^*)$, one can conclude that $\mathbf{P}_{i\varepsilon} = P_{ii} + O(\tilde{\varepsilon}(t))$ is also a positive definite solution.

Theorem 1: *Under assumptions 1-3, the use of a soft constrained Nash equilibrium* $\mathbf{u}_i^{(k)*}(t) = -\mathbf{F}_{i\varepsilon}^{(k)*}\mathbf{x}(t)$ *results in the following condition.*

$$J_i\left(\mathbf{u}_1^{(k)*}, \ldots, \mathbf{u}_N^{(k)*}, \mathbf{x}(0)\right) \approx J_i\left(\mathbf{u}_1^{*}, \ldots, \mathbf{u}_N^{*}, \mathbf{x}(0)\right) + O\left(\tilde{\varepsilon}^{2^k+1}\right). \tag{30}$$

Proof: Due to space constraints, we merely outline the proof. A detailed related analysis can be found in (Mukaidani, 2009; Sagara et al., 2008).

If the iterative strategy is $\mathbf{u}_i^{(k)*}(t) = -\mathbf{F}_{i\varepsilon}^{(k)*}\mathbf{x}(t)$ then the value of the cost function is given by

$$J_i\left(\mathbf{u}_1^{(k)*}, \ldots, \mathbf{u}_N^{(k)*}, \mathbf{x}(0)\right) = \mathbf{x}^T(0)\mathbf{Y}_{i\varepsilon}\mathbf{x}(0), \tag{31}$$

where $\mathbf{Y}_{i\varepsilon}$ is a *positive semi-definite solution* of the following algebraic Riccati equation

$$\mathbf{Y}_{i\varepsilon}\left(\mathbf{A}_\varepsilon - \sum_{\substack{j=1 \\ j\neq i}}^{N}\mathbf{S}_{j\varepsilon}\mathbf{P}_{j\varepsilon}^{(k)}\right) + \left(\mathbf{A}_\varepsilon - \sum_{\substack{j=1 \\ j\neq i}}^{N}\mathbf{S}_{j\varepsilon}\mathbf{P}_{j\varepsilon}^{(k)}\right)^T \mathbf{Y}_{i\varepsilon}$$

$$+ \mathbf{Y}_{i\varepsilon}\mathrm{M}_{i\varepsilon}\mathbf{Y}_{i\varepsilon} + \varepsilon\sum_{\substack{j=1 \\ j\neq i}}^{N}\mathbf{P}_{j\varepsilon}^{(k)}\mathbf{S}_{ij\varepsilon}\mathbf{P}_{j\varepsilon}^{(k)} - \mathbf{P}_{i\varepsilon}^{(k)}\mathbf{S}_{i\varepsilon}\mathbf{P}_{i\varepsilon}^{(k)} + \mathbf{D}_{i\varepsilon}^T\mathbf{D}_{i\varepsilon} = \mathbf{0}. \tag{32}$$

Let $\mathbf{Z}_{i\varepsilon} = \mathbf{Y}_{i\varepsilon} - \mathbf{P}_{i\varepsilon}$; then subtracting SWARRE (26) from (32) satisfies the following equation

$$\mathbf{Z}_{i\varepsilon}\bar{\mathbf{A}}_\varepsilon^{(k)} + \bar{\mathbf{A}}_\varepsilon^{(k)T}\mathbf{Z}_{i\varepsilon} + \sum_{\substack{j=1 \\ j\neq i}}^{N}\mathbf{P}_{i\varepsilon}\mathbf{S}_{j\varepsilon}\left(\mathbf{P}_{j\varepsilon} - \mathbf{P}_{j\varepsilon}^{(k)}\right)$$

$$+ \sum_{\substack{j=1 \\ j\neq i}}^{N}\left(\mathbf{P}_{j\varepsilon} - \mathbf{P}_{j\varepsilon}^{(k)}\right)\mathbf{S}_{j\varepsilon}\mathbf{P}_{i\varepsilon} + \varepsilon\left[\sum_{\substack{j=1 \\ j\neq i}}^{N}\left(\mathbf{P}_{j\varepsilon}^{(k)}\mathbf{S}_{ij\varepsilon}\mathbf{P}_{j\varepsilon}^{(k)} - \mathbf{P}_{j\varepsilon}\mathbf{S}_{ij\varepsilon}\mathbf{P}_{j\varepsilon}\right)\right] + \left(\mathbf{P}_{i\varepsilon} - \mathbf{P}_{i\varepsilon}^{(k)}\right)\mathbf{S}_{i\varepsilon}\left(\mathbf{P}_{i\varepsilon} - \mathbf{P}_{i\varepsilon}^{(k)}\right) = 0, \tag{33}$$

where $\bar{\mathbf{A}}_\varepsilon^{(k)} = \mathbf{A}_\varepsilon - \sum_{j=1}^{N}\mathbf{S}_{j\varepsilon}\mathbf{P}_{j\varepsilon}^{(k)} + \mathbf{M}_{i\varepsilon}\mathbf{P}_{i\varepsilon}^{(k)} + \mathbf{M}_{i\varepsilon}\left(\mathbf{P}_{i\varepsilon} - \mathbf{P}_{i\varepsilon}^{(k)}\right)$. Suppose $\left\|\mathbf{P}_{i\varepsilon} - \mathbf{P}_{i\varepsilon}^{(k)}\right\| \approx O\left(\tilde{\varepsilon}^{2^k}\right)$, (i.e., has a quadratic rate of convergence); then from the proof of theorem 1, one can have,

$$\theta(\mathbf{Z}_{i\varepsilon}) = \mathbf{Z}_{i\varepsilon}\left(\hat{\mathbf{J}} + O(\tilde{\varepsilon})\right) + \left(\hat{\mathbf{J}} + O(\tilde{\varepsilon})\right)^T\mathbf{Z}_{i\varepsilon} + \mathbf{Z}_{i\varepsilon}\mathbf{M}_{i\varepsilon}\mathbf{Z}_{i\varepsilon} + O\left(\tilde{\varepsilon}^{2^k+1}\right) = 0, \tag{34}$$

where $\theta(\mathbf{0}) = O\left(\tilde{\varepsilon}^{2^k+1}\right)$ and $\hat{\mathbf{J}} = \mathbf{block\ diag}\left(\Delta_{11} \ldots \Delta_{NN}\right)$ with $\Delta_{ii} = \mathbf{A}_{ii} - (\mathbf{S}_{ii} - \mathbf{M}_{ii})\mathbf{P}_{ii}$ [258]. Thus, let $\|\mathbf{Z}_{i\varepsilon} - \mathbf{0}\| \leq O\left(\tilde{\varepsilon}^{2^k+1}\right)$ and from the cost function definition it is evident that:

$$\mathbf{x}^T(0)\mathbf{Z}_{i\varepsilon}\mathbf{x}(0) = \mathbf{x}^T(0)\mathbf{Y}_{i\varepsilon}\mathbf{x}(0) - \mathbf{x}^T(0)\mathbf{P}_{i\varepsilon}\mathbf{x}(0)$$

$$= J_i\left(\mathbf{u}_1^{(k)*}, \ldots, \mathbf{u}_N^{(k)*}, \mathbf{x}(0)\right) - J_i\left(\mathbf{u}_1^*, \ldots, \mathbf{u}_N^*, \mathbf{x}(0)\right)$$

$$\leq O\left(\tilde{\varepsilon}^{2^k+1}\right) \quad . \tag{35}$$

5. Simulation tests and results

5.1 Simulation tests

The efficiency of the proposed model and algorithm was studied by means of numerical examples. The MATLAB™ tool was used to evaluate the design optimization parameters, because of its efficiency in numerical computations. The wireless MRMC network being considered was modelled as a large scale interconnected control system. Upto 50 wireless nodes were randomly placed in a 1200 m by 1200 m region. The random topology depicts a non-uniform distribution of the nodes. Each node was assumed to have at most four NICs or radios, each tuned to a separate non-overlapping UCG as shown in Fig. 7. Although 4 radios are situated at each node, it should be noted that such a dimension merely simplifies the simulation. The higher dimension of radios per node may be used without loss of generality. The MRMC configurations depict the weak coupling to each other among different non-overlapping channels. In other words, those radios of the same node operating on separate frequency channels (or UCGs) do not communicate with each other. However, due to their close vicinity such radios significantly interfere with each other and affect the process of optimal power control. The ISM carrier frequency band of 2.427 GHz-2.472 GHz was assumed for simulation purposes only. Figure 7 illustrates the typical wireless network scenario with 4 nodes, each with 4 radio-pairs or users able to operate simultaneously. The rationale is to stripe application traffic over power controlled multiple channels and/or to access the WMCs as well as backhaul network cooperation (Olwal et al., 2009**a**).

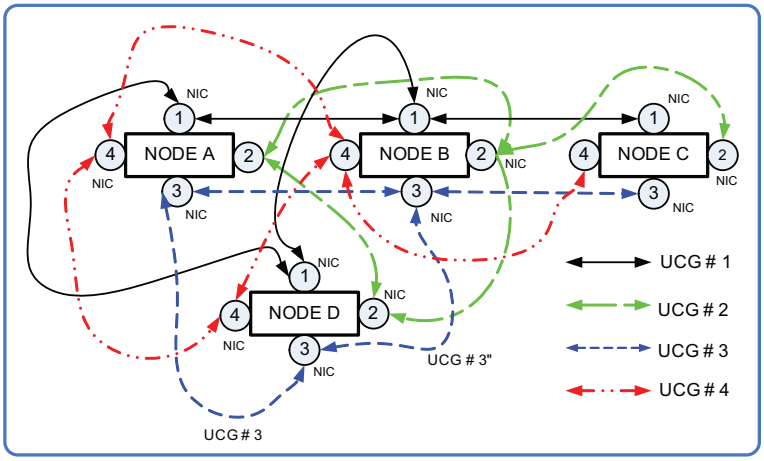

Fig. 7. MRMC wireless network

5.2 Performance evaluation

In order to evaluate the performance of the singularly-perturbed weakly-coupled dynamic transmission power management (TPM) scheme in terms of power and throughput, our simulation parameters, additional to those in section 5.1, were outlined as follows: The Distributed Inter Frame Space (DIFS) time = 50 μs , Short Inter Frame Space (SIFS) time = 10 μs and Back-off slot time = 20 μs . The number of mini-slots in the probe phase, M = 20, duration of probe mini-slot, T_{pc} = 40 μs and ATIM and power selection window adjustment parameter, ϑ = 1.2-1.5 as well as a virtual time-slot duration consisting of probe, power optimization and data packet transmission times, t = 100 ms.

An arrival rate of λ packets/sec of packets at each queue was assumed. For each arriving packet at the sending queue, a receiver was randomly selected from its immediate neighbours. Each simulation run was performed long enough for the output statistics to stabilize (i.e., sixty seconds simulation time). Each datum point in the plots represents an average of four runs where each run exploits a different randomly generated network topology. Saturated transmission power consumption and throughput gain performance were evaluated. Saturation conditions mean that packets are always assumed to be in the queue for transmission; otherwise, the concerned transmitting radio goes to doze/sleep mode to conserve energy (i.e., back-off amount of time).

The following parameters were varied in the simulation: the number of active links (transmit-receive radio-pairs) interfering (i.e., co-channel and cross-channel), from 2 to 50 links, the channels' availability, from 1 to 4 and the traffic load, from 12.8 packets/s to 128 packets/s. The maximum possible power consumed by a radio in the transmit state, the receive state, the idle state and the doze state was assumed as 0.5 Watt, 0.25 Watt, 0.15 Watt and 0.005 Watt, respectively. A user being in the transmitting state means that the radio at the head of the link is in the transmit state while the radio at the tail of the link is in the receive state. A user in the receive state, in the idle state, and in the doze state means that both the radio at the head of the link and the radio at the tail of the link are in the receive state, in the idle state, and in the doze state, respectively (Wang et al., 2006). In order to evaluate the transmission power consumption, packets must be assumed to be always available in all the sending queues of nodes. This is a condition of network saturation.

5.3 Results and disscussions

Figure 8 illustrates an average transmission power per node pair at steady state, versus the number of active radios relative to the total number of adjacent channels. During each time slot, each node evaluates steady state transmission powers in the ATIM phase. Average transmission power was measured as the number of active radio interfaces was increased at different values of the queue perturbations and the weak couplings of the MRMC systems. An increase in the number of active interfaces results in a linear increase in the transmission powers per node-pairs. At 80%, the number of radios relative to the number of adjacent channels with $\varepsilon = \sqrt{|\varepsilon_s \varepsilon_w|} = 0.0001$ yields about 0.61%, 7.98%, 9.51% respectively, a greater power saving than with $\varepsilon = 0.001$, 0.01 and 0.1. This is explained as follows. Stabilizing a highly perturbed queue system and strongly interfered disjoint wireless channels consumes more source energy. Packets are also re-transmitted frequently because of high packet drop rates. Retransmitting copies of previously dropped packets results in perturbations at the queue system owing to induced delays and energy-outages.

A number of previously studied MAC protocols for throughput enhancement were compared with the SPWC-PMMUP based power control scheme. The multi-radio unification protocol (MUP) was compared with the SPWC-PMMUP scheme because the latter is a direct extension of the former in terms of energy-efficiency. Both protocols are implemented at the LL and with the same purpose (i.e., to hide the complexity of the multiple PHY and MAC layers from the unified higher layers, and to improve throughput performance). However, the MUP scheme chooses only one channel with the best channel quality to exchange data and does not take power control into consideration. The power-saving multi-radio multi-channel medium access control (MAC) (PSM-MMAC) was compared with the SPWC-PMMUP scheme, because both protocols share the following characteristics: they are energy-efficient, and they select channels, radios and power states dynamically based on estimated queue lengths, channel conditions and the number of active links. The single-channel power-control medium access control (POWMAC) protocol was compared with the SPWC-PMMUP because both are power controlled MAC protocols suitable for wireless Ad Hoc networks (e.g., IEEE 802.11 schemes). Such protocols perform the carrier sensed multiple access with collision avoidance (CSMA/CA) schemes. Both protocols possess the capability to exchange several concurrent data packets after the completion of the operation of the power control mechanism. Both are distributed, asynchronous and adaptive to changes of channel conditions.

Figure 9 depicts the plots for energy-efficiency versus the number of active links per square kilometre of an area. Energy-efficiency is measured in terms of the steady state transmission power per time slot, divided by the amount of packets that successfully reach the target receiver. It is observed that low active network densities generally provide higher energy-efficiency gain than highly active network densities. This occurs because low active network densities possess better spatial re-use and proper multiple medium accesses. Except for low network densities, the SPWC-PMMUP scheme outperforms the POWMAC, the power saving multi-channel MAC (i.e., PSM-MMAC) and the MUP schemes. In low active network density, a single channel power controlled MAC (i.e., POWMAC) records a higher degree of freedom with spatial re-use. As a result, it indicates a low expenditure of transmission power. As the number of active users increases, packet collisions and retransmissions become significantly large. The POWMAC uses an adjustable access window to allow for a series of RTS/CTS exchanges to take place before several concurrent data packet transmissions can commence. Unlike its counterparts, the POWMAC does not make use of control packets (i.e., RTS/CTS) to silence neighbouring terminals. Instead, collision avoidance information is inserted in the control packets and is used in conjunction with the received signal strength of these packets to dynamically bound the transmission power of potentially interfering terminals in the vicinity of a receiving terminal. This allows an appropriate selection of transmission power that ensures multiple-concurrent transmissions in the vicinity of the receiving terminal. On the other hand, both SPWC-PMMUP and PSM-MMAC contain an adjustable ATIM window for traffic loads and the LL information. The ATIM window is maintained moderately narrow in order that less energy is wasted owing to its being idle. Statistically, the simulation results indicated that for between 4 and 16 users per deployment area, the POWMAC scheme was on average 50%, 87.50%, and 137.50% more energy-efficient than the SPWC-PMMUP, PSM-MMAC and MUP, respectively. However, between 32 and 50 users per deployment area, in the SPWC-PMMUP scheme, yielded on average 14.58%, 66.67%, and 145.83% more energy efficiency than the POWMAC, PSM-MMAC and MUP schemes, respectively.

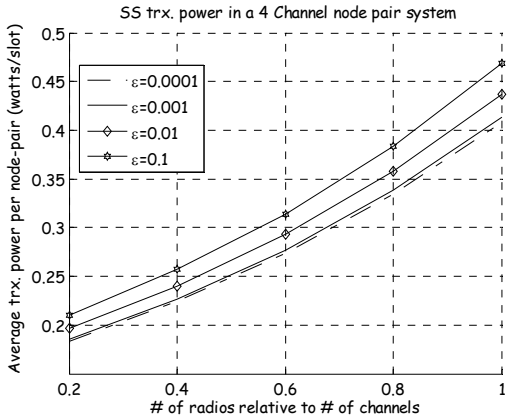

Fig. 8. Steady state transmission power versus relative number of radios per channel

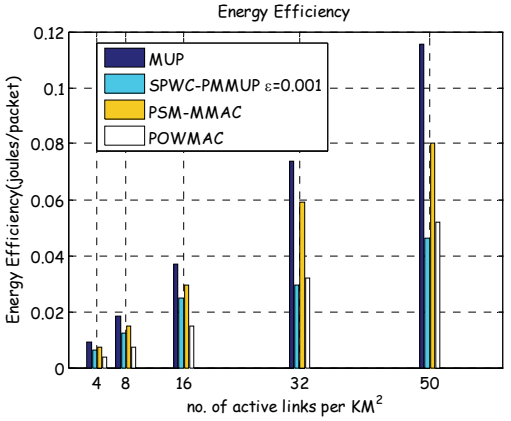

Fig. 9. Energy-efficiency versus density of active links

Figure 10 depicts the performance of the network lifetime observed for the duration of the simulation. The number of active links using steady state transmission power levels was initially assumed to be 36 links per square kilometre of area. Under the saturated traffic generated by the queue systems, different protocols were simulated and compared to the SPWC-PMMUP scheme. The links which were still alive were defined as those which were operating on certain stabilized transmission power levels and which remained connected at the end of the simulation time. The SPWC-PMMUP scheme evaluates the network lifetime based on the stable connectivity measure. That is, if a transmission power level, $p_{ij} = p_{ij}^*$ then the link (i, j) exists; otherwise if $p_{ij} < p_{ij}^*$, then there is no link between the transmitting interface i and the receiving interface j (i.e., the tail of the link). The notation, p_{ij}^* represents the minimum transmission power level needed to successfully send a packet to the target receiver at the immediate neighbours. After 50 units of simulation time, the SPWC-PMMUP scheme records, on average, 12.50%, 22.22% and 33.33%, of links still alive, more than the POWMAC, PSM-MMAC and MUP schemes, respectively. This is because

SPWC-PMMUP scheme uses a fractional power to perform the medium access control (i.e., RTS/CTS control packets are executed at a lower power than the maximum possible) while the conventional protocols employ maximum transmission powers to exchange control packets. The SPWC-PMMUP also transmits application or data packets using a transmission power level which is adaptive to queue perturbations, the intra and inter-channel interference, the receiver SINR, the wireless link rate and the connectivity range. The performance gains of the POWMAC scheme are explained as follows. The POWMAC uses a collision avoidance inserted in the control packets, and in conjunction with the received signal strength of these packets, to dynamically bound the transmission powers of potentially interfering terminals in the vicinity of a receiving terminal. This promotes mutual multiple transmissions of the application packets at a controlled power over a relatively long time. The PSM-MMAC scheme offers the desirable feature of being adaptive to energy, channel, queue and opportunistic access. However, its RTS/CTS packets are executed on maximum power. The MUP scheme does not perform any power control mechanism and hence records the worst lifetime performance.

Figure 11 illustrates an average throughput performance versus the offered traffic load at different singular-perturbation and weak-coupling conditions. Four simulation runs were performed at different randomly generated network topologies. The average throughput per send and receive node-pairs was measured when packets were transmitted using steady state transmission powers. Plots were obtained at confidence intervals of 95%, that is, with small error margins. In general, the average throughput monotonically increases with the amount of the traffic load subjected to the channels. The highly-perturbed and strongly-coupled multi-channel systems, that is, $\varepsilon = \sqrt{|\varepsilon_s \varepsilon_w|} = 0.1$, degrade average per hop throughput performance compared to the lowly-perturbed and weakly-coupled system, that is, $\varepsilon = 0.0001$. On average, and at 100 packets/s of the traffic load, the system described by $\varepsilon = 0.0001$ can provide 4%, 16% and 28% more throughput performance gain over the system at $\varepsilon = 0.001$, $\varepsilon = 0.01$ and $\varepsilon = 0.1$, respectively. This may be explained as follows. In large queue system perturbations (i.e., $\varepsilon = 0.1$) the SPWC-PMMUP scheme wastes a large portion of the time slot in stabilizing the queue and in finding optimal transmission power

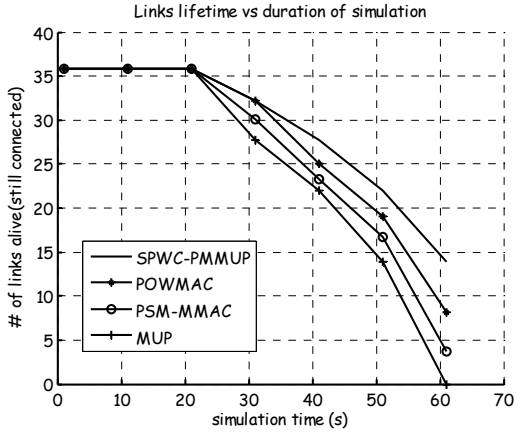

Fig. 10. Active links lifetime performance

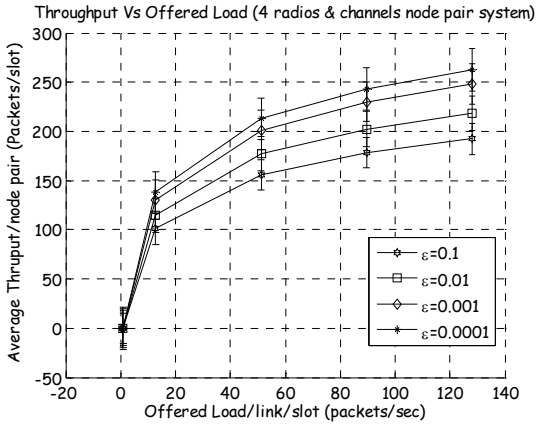

Fig. 11. Average Throughput versus offered Load

levels. This means that only lesser time intervals are allowed for actual application packet transmission. Furthermore, the inherently high inter-channel interference degrades the spatial re-use. Consequently, smaller volumes of application/data packets actually reach the receiving destination successfully (i.e., low throughput). Conversely, with a low perturbation and inter-channel interference (i.e., $\varepsilon = 0.001$), data packets have a larger time interval for transmission; the wireless medium is spectrally efficient and hence achieves an enhanced average throughput.

6. Conclusion

This chapter has furnished an optimal TPM scheme suitable for backbone wireless mesh networks employing MRMC configurations. As a result, an energy-efficient link-layer TPM called SPWC-PMMUP has been proposed for a wireless channel with packet losses. The optimal TPM demonstrated at least 14% energy-efficiency and 28% throughput performance gains over the conventional schemes, in less efficient channels (Figs. 9 & 11). However, a joint TPM, channel and routing optimization for MRMC wireless networks remains an open issue for future investigation.

7. References

Adya, A.; Bahl, P.; Wolman, A. & Zhou, L. (2004). A multi-radio unification protocol for IEEE 802.11 wireless networks, *Proceedings of international conference on broadband networks (Broadnets'04)*, pp. 344-354, ISBN: 0-7695-2221-1, San Jose, October 2004, IEEE, CA.

Akyildiz, I. F. & Wang, X. (2009). *Wireless mesh networks*, John Wiley & Sons Ltd, ISBN: 978-0-470-03256-5, UK.

El-Azouzi, R. & Altman, E. (2003). Queueing analysis of link-layer losses in wireless networks, *Proceedings of personal wireless communications*, pp. 1-24, ISBN: 3-540-20123-8, Venice, September 2003, Italy.

Gajic, Z. & Shen, X. (1993). *Parallel algorithms for optimal control of large scale linear systems,* Springer-Verlag, ISBN: 3-540-19825-3, New York.

Iqbal, A. & Khayam, S. A. (2009). An energy-efficient link-layer protocol for reliable

transmission over wireless networks. *EURASIP journal on wireless communications and networking,* Vol. 2009, No. 10, July 2009, ISSN: 1687-1472.

Li, D.; Du, H.; Liu, L. & Huang, S. C.-H. (2008). Joint topology control and power conservation for wireless sensor networks using transmit power adjustment, In: *Computing and combinatorics*, X. Hu & J. Wang (Eds.), pp. 541-550, Springer Link, ISBN: 978-3-540-69732-9, Berlin.

Li, X.; Cao, F. & Wu, D. (2009). QoS-driven power allocation for multi-channel communication under delayed channel side information, *Proceedings of consumer communications & networking conference*, ISBN: 978-952-15-2152-2, Las Vegas, January 2009, Nevada, USA.

Maheshwari, R.; Gupta, H. & Das, S. R. (2006). Multi-channel MAC protocols for wireless networks, *Proceedings of IEEE SECON 2006*, ISBN: 978-1-580-53044-6, Reston, September 2006, IEEE, VA.

Merlin, S.; Vaidya, N. & Zorzi, M. (2007). *Resource allocation in multi-radio multi-channel multi-hop wireless networks,* Technical Report: 35131, July 2007, Padova University.

Mukaidani, H. (2009). Soft-constrained stochastic Nash games for weakly coupled large-scale systems. *Elsevier automatica*, Vol. 45, pp. 1272-1279, 2009, ISSN: 0005-1098.

Muqattash, A. & Krunz, M. (2005). POWMAC: A single-channel power control protocol for throughput enhancement in wireless ad hoc networks. *IEEE journal on selected areas in communications*, Vol. 23, pp. 1067-1084, 2005, ISSN: 0733-8716.

Olwal, T. O.; Van Wyk, B. J; Djouani, K.; Hamam, Y.; Siarry, P. & Ntlatlapa, N. (2009a). Autonomous transmission power adaptation for multi-radio multi-channel WMNs, In: *Ad hoc, mobile and wireless networks*, P. M. Ruiz & J. J. Garcia-Luna-Aceves (Eds.), pp. 284-297, Springer Link, ISBN: 978-3-642-04382-6, Berlin.

Olwal, T. O.; Van Wyk, B. J; Djouani, K.; Hamam, Y.; Siarry, P. & Ntlatlapa, N. (2009b). A multi-state based power control for multi-radio multi-channel WMNs. *International journal of computer science*, Vol. 4, No. 1, pp. 53-61, 2009, ISSN: 2070-3856.

Olwal, T. O.; Van Wyk, B. J; Djouani, K.; Hamam, Y. & Siarry, P. (2010a). Singularly-perturbed weakly-coupled based power control for multi-radio multi-channel wireless networks. *International journal of applied mathematics and computer sciences,* Vol. 6, No. 1, pp. 4-14, 2010, ISSN: 2070-3902.

Olwal, T. O.; Van Wyk, B. J; Djouani, K.; Hamam, Y.; Siarry, P. & Ntlatlapa, N. (2010b). Dynamic power control for wireless backbone mesh networks: a survey. *Network protocols and algorithms,* Vol. 2, No. 1, pp. 1-44, 2010, ISSN: 1943-3581.

Park, H.; Jee, J. & Park, C. (2009). Power management of multi-radio mobile nodes using HSDPA interface sensitive APs, *Proceedings of IEEE 11th international conference on advanced communication technology*, pp. 507-511, ISBN: 978-89-5519-139-4, Phoenix Park, South Korea, February 2009.

Sagara, M.; Mukaidani, H. & Yamamoto, T. (2008). Efficient numerical computations of soft-constrained Nash strategy for weakly-coupled large-scale systems. *Journal of computers*, Vol. 3, pp. 2-10, November 2008, ISSN: 1796-203X.

Thomas, R. W.; Komali, R. S.; MacKenzie, A. B. & DaSilva, L. A. (2007). Joint power and channel minimization in topology control: a cognitive network approach, *Proceedings of IEEE international conference on communication*, pp. 6538-6542, ISBN: 0-7695-2805-8, Glasgow, Scotland, 2007.

Wang, J.; Fang, Y. & Wu, D. (2006). A power-saving multi-radio multi-channel MAC

protocol for wireless local area networks, *Proceedings of IEEE infocom 2006 conference*, pp. 1-13, ISBN: 1-4244-0222-0, Barcelona, Spain, 2006.

Zhou, H.; Lu, K. & Li, M. (2008). Distributed topology control in multi-channel multi-radio mesh networks, *Proceedings of IEEE international conference on communication*, ISBN: 0-7803-6283-7, New Orleans, USA, May 2008.